

Incoherent interaction of propagating spin waves with precessing magnetic momentsB. C. Choi,¹ E. Girgis,¹ C. A. Ross,² Th. Speliotis,³ Y. K. Hong,⁴ G. S. Abo,⁴ D. Niarchos,³ and H. Miyagawa^{2,*}¹*Department of Physics and Astronomy and Centre for Advanced Materials and Related Technology (CAMTEC), University of Victoria, Victoria, British Columbia, Canada V8W 3P6*²*Department of Materials Science and Engineering, Massachusetts Institute of Technology, Cambridge, Massachusetts 02139, USA*³*Institute of Materials Science, NCSR "Demokritos," 15310 Aghia Paraskevi, Greece*⁴*Department of Electrical and Computer Engineering and MINT Center, University of Alabama, Tuscaloosa, Alabama 35487, USA*

(Received 30 October 2009; revised manuscript received 17 February 2010; published 23 March 2010)

The magnetization dynamics of the magnetic vortex state occurring in response to subnanosecond transitions of the externally applied magnetic field was investigated in Ni₈₀Fe₂₀(12 nm)/Ir₈₀Mn₂₀(5 nm) square elements by exploiting time-resolved scanning Kerr microscope and micromagnetic modeling. Upon application of a magnetic field pulse the magnetization undergoes a precessional oscillation of ~ 2 GHz while the magnetic vortex core moves from the equilibrium position. Along the pathway of the moving core, strong bursts of spin waves are generated by the creation and subsequent annihilation of a vortex-antivortex pair. An abrupt suppression of magnetization precession occurs subsequently after a vortex-antivortex core annihilates. The observed suppression is attributed to the incoherent interaction of precessing magnetic moments with propagating spin waves. The experimental observations are qualitatively well reproduced by micromagnetic modeling.

DOI: [10.1103/PhysRevB.81.092404](https://doi.org/10.1103/PhysRevB.81.092404)

PACS number(s): 75.60.Ch, 75.70.Ak, 75.70.Kw

Over the last few years, the study of nonequilibrium magnetization phenomena in microscale and nanoscale magnets has attracted the attention of a number of research groups.^{1–4} In particular, the magnetic properties in patterned circular disks and square elements have attracted much interest due to their fundamental importance and their future technological applications in high-speed magnetoelectronic devices. The remanent magnetization configuration of square elements, for example, has a typical Landau-type structure with four triangular domains separated by 90° domain walls.⁵ The magnetization forms a vortex core at the center of the domain structure, where the four domains meet one another. As magnetic vortex structures are energetically very stable and have low stray fields, these structures have been considered as the ideal candidates for high-density integration.^{6–9} One interesting discovery found in magnetic elements with a vortex state is the dynamic core switching mediated by the formation of a vortex-antivortex pair and their subsequent annihilation.^{6,7,10} A striking feature of the vortex-core dynamics is that the vortex-antivortex pair formation is initiated by the dynamic deformation of the vortex core. Recently, Vansteenkiste *et al.*¹¹ experimentally revealed the details of the vortex-core deformation upon application of magnetic field pulse by using time-resolved magnetic x-ray microscopy. Another interesting phenomenon occurring in the magnetization dynamics in vortex structures is the radiation of spin waves generated by the annihilation of a vortex-antivortex pair.^{6,7} In a recent report, it has been discussed that the emission of spin waves may play an important role in magnetic damping processes.⁹ Here we report a pathway for effectively suppressing the magnetization precession in a Landau-shaped vortex structure, in which the incoherent interaction of precessing magnetic moments with propagating spin waves plays a critical role. This mechanism has not been explored yet, and can be accessed via time-resolved probing as demonstrated in this Brief Report.

In our experiments, the polycrystalline Ni₈₀Fe₂₀(12 nm)/Ir₈₀Mn₂₀(5 nm)/Ta(5 nm) samples were prepared as an array of square elements with 10 μm lengths

onto 15- μm -thick glass substrates by optical lithography, lift-off, and dc-triode sputtering deposition. The samples were then heated to 600 K, which is above the Néel temperature of Ir₈₀Mn₂₀, and subsequently cooled to room temperature in the presence of the magnetic field of 15 Oe. First the quasistatic magnetization properties was studied by measuring hysteresis loops of individual square elements using magneto-optical Kerr effect, in which the external magnetic field of ± 100 Oe sweeps at a slow rate of ~ 1 Hz. As shown in Fig. 1(a), the shape of the loops is typical for the magnetization curve of a vortex structure, in which the nucleation and annihilation fields of the vortex core are measured $H_n = 14$ Oe and $H_a = 60$ Oe, respectively. The hysteresis loop is shifted along the cooling field direction due to the presence of the induced exchange-bias field (H_{ex}) of 8 Oe. Magnetization dynamics is studied by using a time-resolved scanning Kerr microscope with a spatial resolution (Rayleigh criterion) of ~ 800 nm. As schematically illustrated in Fig. 1(b), square elements are mounted on top of the 20- μm -wide and 300-nm-thick Au microcoil, which is used to generate fast magnetic field pulses (H_s) along an edge of the element.¹² The field strength of H_s is ~ 60 Oe with a duration of 4.5 ns. Its rise and fall times are 250 ps and 500 ps, respectively. Also shown in the inset is the profile of H_s , which was measured by directly probing the current pulse using a fast sampling oscilloscope. The magnetic pulses are synchronously triggered by a mode-locked Ti-sapphire femtosecond laser (tuned to $\lambda = 780$ nm) at a 0.8 MHz repetition rate. The experimental setup based on pump-and-probe technique is described in detail elsewhere.¹² A typical measurement of the temporal evolution of the magnetization component M_x is shown in Fig. 1(b), in which the magneto-optical signal was averaged over the area of the probe spot positioned close to the center of the element. Upon application of a magnetic field pulse, the average magnetization rapidly undergoes a large angle switching toward the direction of H_s , which is the $+x$ axis in our experimental configuration. Following its initial rapid switching, the magnetization under-

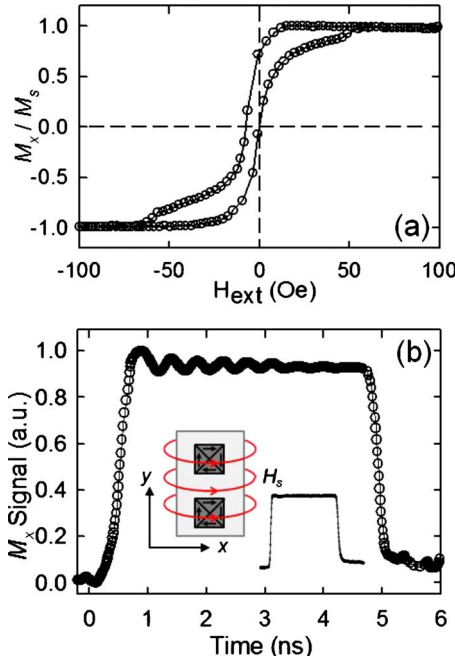


FIG. 1. (Color online) (a) Hysteresis loop measured using magneto-optical Kerr effect setup. The in-plane magnetic field is applied along the exchange-bias field direction. (b) Time-resolved measurement of the magnetization component M_x along the applied magnetic field pulse direction. (Inset) A schematic of the $\text{Ni}_{80}\text{Fe}_{20}$ square elements placed on top of the Au wire. Also shown is the profile of switching field pulse H_s , which was obtained by directly probing the current pulse.

goes precessional motion, as manifested by the presence of the oscillation of M_x .

Figure 2(a) shows an expanded view of the temporal evolution of M_x , shown in Fig. 1(b). Clear evidence of a damped oscillatory motion of M_x is found. The precessional frequency of 2.2 GHz is determined from the Fourier transformation, as shown as the black curve in Fig. 2(b). We note that the vortex dynamics is found to be strongly dependent on the exchange-bias field strength (H_{ex}), in which a shift to a lower precessional frequency has been observed as H_{ex} increases. A full discussion about the dependence of the vortex dynamics on H_{ex} will be given elsewhere.¹³ A very interesting point found in the temporal evolution of M_x is the abrupt drop of the precessional amplitude after a few full cycles of oscillation. A careful examination of the $M_x(t)$ curve resolves the abrupt drop occurring at 3.3 ns, which was confirmed in subsequently repeated measurements. In order to examine the influence of the abrupt drop of the precessional amplitude on the resonance frequency, fast Fourier transform (FFT) spectra obtained from $M_x(t)$ before and after the abrupt suppression of the precession are compared in Fig. 2(b), but no significant shift of the peaks for presuppression (red curve, $1.25 \text{ ns} < t < 3.30 \text{ ns}$) and postsuppression (blue curve, $3.30 \text{ ns} < t < 4.25 \text{ ns}$) is found. This implies that a resonance mode of $\sim 2.2 \text{ GHz}$ is excited in response to a magnetic field pulse and remains throughout the magnetization process.

Detailed understanding of the magnetization dynamics of the vortex state can be obtained by capturing the time evo-

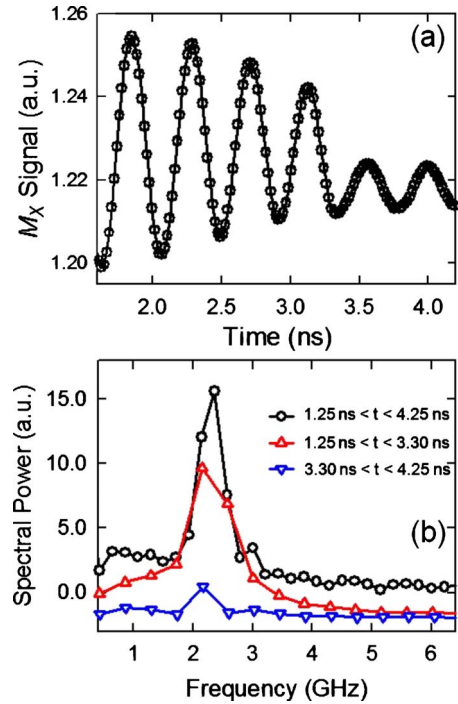


FIG. 2. (Color online) (a) Expanded view of the time traces of magnetization component M_x , shown in Fig. 1(b). Magnetization precession is accompanied by an abrupt suppression of the precessional amplitude at $\sim 3.3 \text{ ns}$. (b) Fourier spectrum amplitude as a function of frequency. The black curve is obtained from $M_x(t)$ for $1.25 < t < 4.25 \text{ ns}$ while the red (triangle-up symbols) and blue (triangle-down symbols) curves are from $M_x(t)$ before and after the suppression, respectively.

lution of the domain configuration in response to short magnetic pulses. Figure 3 shows a series of the nonequilibrium magnetization configurations captured at selected time points. The numbers below the images indicate the time after a magnetic field pulse is applied at $t=0 \text{ ns}$. The contrast in the images reflects the local magnetization configuration, with red areas corresponding to the longitudinal components of the magnetization along $+x$ direction (M_x), whereas blue areas are $-M_x$ regions. The white arrows in the image are to help visualize the four in-plane magnetization domains

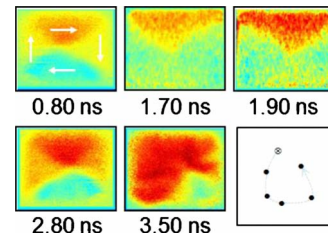


FIG. 3. (Color online) Nonequilibrium magnetization configuration of M_x at selected time points after the onset of a magnetic field pulse at $t=0 \text{ ns}$. The white arrows in the first image are to help visualize the in-plane magnetization around the vortex core. Red (dark contrast in print) corresponds to $+M_x$ component. The last panel shows a circulating trajectory, a gyrotropic motion, of the vortex core. The area shown is $1 \mu\text{m} \times 1 \mu\text{m}$. The position of the vortex core captured at 0.14 ns after the application of a magnetic field pulse is marked by the symbol \otimes .

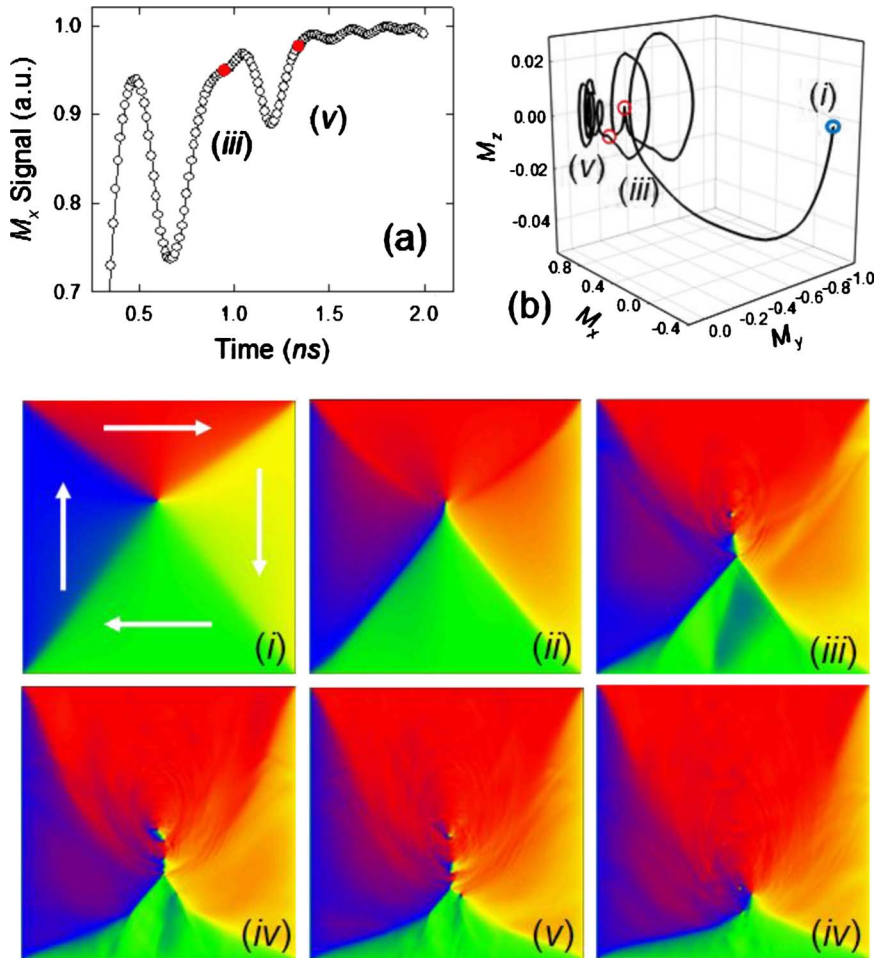


FIG. 4. (Color online) (a) Micromagnetic simulation of time trace of magnetization component M_x after a magnetic field pulse of 70 Oe is applied. An abrupt suppression of the precessional amplitude is reproduced. (b) 3D trajectory of \mathbf{M} after the application of a magnetic field pulse. The initial point of \mathbf{M} prior to the pulse excitation is denoted as a blue dot. Note that the M_z component is enlarged for clarity. (Bottom panel) A series of the nonequilibrium states of M_x with increasing time. The full scope of the dynamic evolution can be seen in movie (Ref. 21).

around the vortex core. The domain image captured at the initial stage of the excitation ($t=0.8$ ns), reveals a Landau-type vortex structure. With increasing time, an oscillatory behavior of the domain wall is observed, in which the bulging of the domain wall in the top quadrant occurs at 1.7 ns, as previously discussed by Raabe *et al.*¹⁴ The domain-wall bulging is subsequently reversed (1.9 ns). In addition to the domain-wall motion, an excitation mode of the vortex core, the so-called gyrotropic mode, is observed. Even though the position of the vortex core is not directly accessible due to the limited spatial resolution, the trajectory of vortex-core motion can be traced by locating the intersection of the contrast between domains. In the last panel of Fig. 3, the core positions are traced for the time interval between 0.14 and 2.8 ns in the center portion of the element. The initial displacement of the vortex core is found to be perpendicular to the applied field pulse direction.¹⁴ After the initial displacement, the vortex core carries out a counterclockwise (CCW) gyrotropic motion.^{14–16} The sense of the gyrotropic motion depends on the out of plane magnetization of the vortex core and the CCW trajectory of the core motion indicates that the core magnetization is out of plane in the positive z direction.¹⁵ Since the core circulation direction remains in the same sense throughout the time period traced, the core magnetization is concluded not to flip throughout the dynamic process up to 2.8 ns.¹⁰ After $t=2.8$ ns, a considerable part of the element becomes magnetized along the applied

field (H_x) direction and it becomes difficult to locate the vortex-core position. We note that the gyrotropic motion is a low-frequency mode with the typical eigenfrequency of sub-gigahertz regime.^{17–19} The gyrotropic mode cannot be resolved in the FFT spectrum [Fig. 2(b)], and is estimated to about 300 MHz by examining the vortex-core motion illustrated in Fig. 3.

In order to shed light into the physical origin of the observed abrupt suppression of the magnetization precession, micromagnetic finite-element modeling based on the Landau-Lifshitz-Gilbert equation was carried out. A permalloy square element with 3 μm length and 10 nm thickness was subdivided into homogeneously magnetized unit cells of the dimension of $5 \times 5 \times 5 \text{ nm}^3$. It is important to keep the size of the unit cell close to the exchange length in order to fully resolve the structure of the magnetization near the vortex core. The material parameters used in the modeling were: magnetization saturation ($M_S=800 \text{ kA/m}$), exchange stiffness ($A=13 \times 10^{12} \text{ J/m}$), and the damping constant ($\alpha=0.01$). In order to mimic the experimental magnetic field condition, the experimentally obtained pulse profile, shown in the inset of Fig. 1(b), was used in the modeling. The spatiotemporal evolution of the magnetization configuration in response to a 70 Oe strong magnetic field pulse is shown in the bottom panel in Fig. 4. Note that the size of the modeled element is smaller than the real sample to keep the computing time within reasonable limits. Therefore, the strength

of switching field pulse needed to generate bursts of spin waves is not necessarily the same for experiments and modeling. Prior to the application of the field pulse [frame (i) for $t=0$ ns], the magnetization state shows an off-centered vortex due to the presence of the exchange bias field of -10 Oe included in the modeling. After the magnetic pulse is applied, the domain walls respond very quickly and move toward the element center, as shown in the frame (ii). The vortex core, however, has a lower mobility and lags behind the moving domain walls, and as a consequence a long domain-wall forms [frames (ii) and (iv)], which is in accordance with a previous report.²⁰ With increasing time the vortex core is separated from the fast moving domain walls, and subsequently a burst of spin waves is generated through the vortex-antivortex annihilation process, frames (iii) and (v). The full scope of the vortex-core dynamics and spin-wave generation can be seen in movies.²¹

The influence of propagating spin wave on precessing magnetic moments is clearly related to the temporal change in the magnetization. Figure 4(a) shows the temporal response of the magnetization component M_x averaged over an area with the diameter of 300 nm near the center of the element. $M_x(t)$ exhibits the qualitative characteristic of the strongly damped precessional oscillation of the magnetization. The most striking feature reproduced in the modeling is the abrupt suppressions of the precessional oscillation, occurring at the time points denoted as (iii) and (v) in Fig. 4(a). Examining the magnetization configurations captured at these time points, the timing of the abrupt suppressions closely correlates with the generation of strong spin waves. The influence of the propagating spin waves on the magnetization precession is also more clearly observable in the

three-dimensional (3D) trajectory of \mathbf{M} [Fig. 4(b)]. One observes that the magnetization initially precesses through a large angle after the excitation. At the time point (iii), however, the precessional trajectory is heavily quenched, implying that the precessing magnetic moments are strongly disturbed by burstlike spin-wave emission. After (v), the amplitude of the precession is reduced quickly after the second burst of spin waves are generated and propagated through the element. The result clearly supports the assumption that the incoherent interaction of the magnetic moments with the propagating spin waves leads to an effective suppression of the magnetization precession.

In conclusion, magnetization dynamics in vortex structures in response to a short magnetic field pulse is found to be a complex mixture of magnetization precession, domain-wall bulging, and gyrotropic motion of the vortex core. In particular, an abrupt suppression of the precessional amplitude is observed. The observed magnetization dynamics is clearly different from the previously reported beating in which the oscillation amplitude is modulated due to multiple normal modes of different frequencies.²² Careful numerical examination of the spatiotemporal evolution of the magnetization dynamics confirms that the incoherent interaction of precessing magnetic moments with propagating spin waves generated through the vortex-antivortex annihilation process is responsible for the suppression. The result not only supports the previously reported spin-wave generation due to vortex-antivortex annihilation^{6,7,10,11} but also reveals a new mechanism for the suppression of the magnetization precession.

CAR acknowledges the support of the National Science Foundation.

*Department of Advanced Materials Science, Kagawa University, 2217-20 Hayashi-Cho, Takamatsu Kagawa, 761-0396, Japan.

¹K. Yamada, S. Kasai, Y. Nakatani, K. Kobayashi, H. Kohno, A. Thiaville, and T. Ono, *Nature Mater.* **6**, 270 (2007).

²F. Romanens, J. Vogel, W. Kuch, K. Fukumoto, J. Camarero, S. Pizzini, M. Bonfim, and F. Petroff, *Phys. Rev. B* **74**, 184419 (2006).

³V. V. Kruglyak, P. S. Keatley, R. J. Hicken, J. R. Childress, and J. A. Katine, *Phys. Rev. B* **75**, 024407 (2007).

⁴B. C. Choi, J. Ho, G. Arnup, and M. R. Freeman, *Phys. Rev. Lett.* **95**, 237211 (2005).

⁵Q. F. Xiao, J. Rudge, B. C. Choi, Y. K. Hong, and G. Donohoe, *Appl. Phys. Lett.* **89**, 262507 (2006).

⁶R. Hertel and C. M. Schneider, *Phys. Rev. Lett.* **97**, 177202 (2006).

⁷B. C. Choi, J. Rudge, E. Girgis, J. Kolthammer, Y. K. Hong, and A. Lyle, *Appl. Phys. Lett.* **91**, 022501 (2007).

⁸R. Lehdorff, D. E. Bürgler, S. Gliga, R. Hertel, P. Grünberg, and C. M. Schneider, *Phys. Rev. B* **80**, 054412 (2009).

⁹G. Eilers, M. Luettich, and M. Muenzenberg, *Phys. Rev. B* **74**, 054411 (2006).

¹⁰B. Van Waeyenberge *et al.*, *Nature (London)* **444**, 461 (2006).

¹¹A. Vansteenkiste *et al.*, *Nat. Phys.* **5**, 332 (2009).

¹²B. C. Choi and M. R. Freeman, in *Nonequilibrium Spin Dynamics by Time-Resolved Magneto-Optical Kerr Microscope*, in *Ultrafast Magnetic Structures IV*, edited by B. Heinrich and J. A. C. Bland (Springer-Verlag, Heidelberg, 2004).

¹³E. Girgis *et al.* (unpublished).

¹⁴J. Raabe, C. Quitmann, C. H. Back, F. Nolting, S. Johnson, and C. Buehler, *Phys. Rev. Lett.* **94**, 217204 (2005).

¹⁵S. B. Choe, Y. Acremann, A. Scholl, A. Bauer, A. Doran, J. Stöhr, and H. A. Padmore, *Science* **304**, 420 (2004).

¹⁶K. Y. Guslienko *et al.*, *J. Appl. Phys.* **91**, 8037 (2002).

¹⁷X. Zhu, Z. Liu, V. Metlushko, P. Gruetter, and M. R. Freeman, *Phys. Rev. B* **71**, 180408(R) (2005).

¹⁸J. Park, P. Eames, D. M. Engebretson, J. Berezovsky, and P. A. Crowell, *Phys. Rev. B* **67**, 020403(R) (2003).

¹⁹O. G. Heinonen, D. K. Schreiber, and A. K. Petford-Long, *Phys. Rev. B* **76**, 144407 (2007).

²⁰R. Hertel and J. Kirschner, *J. Magn. Magn. Mater.* **270**, 364 (2004).

²¹Movie is available at <http://web.uvic.ca/~bchoi/spinwave.htm>

²²A. Barman, V. V. Kruglyak, R. J. Hicken, J. M. Rowe, A. Kundrotaite, J. Scott, and M. Rahman, *Phys. Rev. B* **69**, 174426 (2004).